

Key Processes and Parameters in a Generic Clay Disposal System Model

2012 American Nuclear Society Winter Meeting, San Diego

Kathryn D. Huff^{1,2} & W. Mark Nutt²

¹University of Wisconsin-Madison & ²Argonne National Laboratory

November 13, 2012





Outline

① Introduction

② Results

③ Summary



Clay Generic Disposal System Model

Sensitivity analysis based on the detailed computational **Clay Generic Disposal System Model (GDSM)** developed by the Used Fuel Disposition (UFD) campaign [2]. was performed with respect to various **key processes and parameters** affecting long-term post-closure performance of geologic repositories in **clay** media.



Clay Generic Disposal System Model

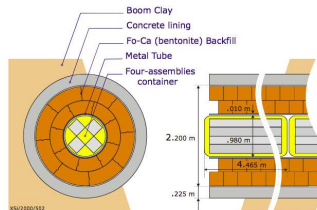


Figure 1 : Belgian reference concept in Boom Clay [8].

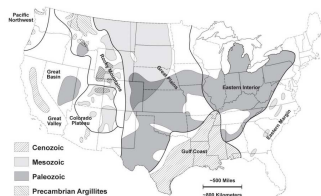


Figure 2 : U.S. Clay Deposits, ref. [5].



Clay Generic Disposal System Model

The Clay GDSM, developed at Argonne National Lab, is built on the GoldSim simulation framework and contaminant transport model. It simulates chemical and physical attenuation processes [4, 3], including

- chemical and physical attenuation processes including
- radionuclide solubility,
- dispersion phenomena,
- and reversible sorption.

Input parameters include

- geometry specifications (e.g. repository depth),
- geologic material properties (e.g. clay porosity),
- geochemical data (e.g. elemental solubility limits),
- and environmental parameters (e.g. natural system velocity).



Clay Generic Disposal System Model

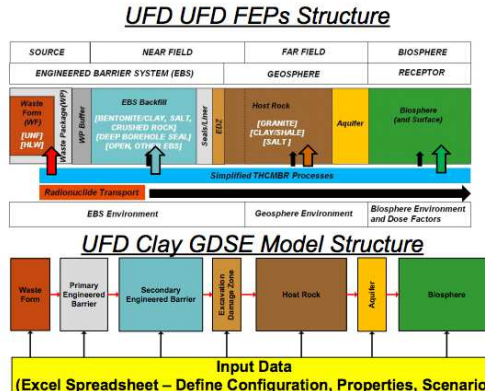


Figure 3.3-2. Clay Long-Term Repository Performance GDS Model Linkages

Figure 3 : General Features Events and Processes in the Clay repository model ??.



Clay Generic Disposal System Model

The disposal concept modeled by the Clay GDSTM [6] is

- an array of spent nuclear fuel packages
- emplaced horizontally
- in excavated tunnels,
- backfilled by a reducing bentonite clay,
- within a clay repository environment,
- **500 meters** beneath the earth's surface.



Mean of the Peak Annual Dose

In this analysis, repository performance is quantified by radiation dose to a hypothetical receptor. Specifically, the mean of the peak annual dose,

$$D_{MoP,i} = \frac{\sum_{r=1}^N \max [D_{r,i}(t)|_{\forall t}]}{N} \quad (1)$$

where

$D_{MoP,i}$ = mean of peak annual dose due to isotope i [$mrem/yr$]

$D_{r,i}(t)$ = year t dose in realization r due to isotope i [$mrem/yr$]

N = number of realizations,

is a conservative metric of repository performance and should not be confused with the peak of the mean annual dose.

$$D_{PoM,i} = \max \left[\frac{\sum_{r=1}^N D_{r,i}(t)|_{\forall t}}{N} \right] \quad (2)$$

= peak of the mean annual dose due to isotope i [$mrem/yr$].



Sampling Strategy

To develop a many dimensional overview, both individual and dual parametric cases were performed.

- **Individual parameter cases** varied a single parameter of interest in detail over a broad range of values.
- **Dual parameter cases** were performed for pairs of parameters expected to exhibit some covariance.

For each case, forty simulation groups varied the parameter or parameters within the range considered. For each simulation group, a 100 realization simulation was completed [2, 6].

Simulation Cases

Case	Parameter	Units	Min. Value	Max. Value
I	D_{eff}	$[m^2 \cdot s^{-1}]$	10^{-8}	10^{-5}
	Inventory	[MTHM]	10^{-4}	10^1
II	$V_{adv,y}$	$[m \cdot yr^{-1}]$	6.31×10^{-8}	6.31×10^{-4}
	D_{eff}	$[m^2 \cdot s^{-1}]$	10^{-8}	10^{-5}
III	S_i	$[mol \cdot m^{-3}]$	$(1 \times 10^{-9})\langle S_i \rangle$	$(5 \times 10^{10})\langle S_i \rangle$
IV	$K_{d,i}$	$[m^3 \cdot kg^{-1}]$	$(1 \times 10^{-9})\langle K_{d,i} \rangle$	$(5 \times 10^{10})\langle K_{d,i} \rangle$
V	$R_{WFDeg.}$	$[yr^{-1}]$	10^{-9}	10^{-2}
	Inventory	[MTHM]	10^{-4}	10^1
VI	t_{WPFail}	[yr]	10^3	10^7
	D_{eff}	$[m^2 \cdot s^{-1}]$	10^{-8}	10^{-5}

Table 1 : Each dual and single parameter simulation case had 40 simulation groups of 100 realizations each.



Outline

① Introduction

② Results

③ Summary



Case I : Diffusion Coefficient and Inventory

Simulation Cases

Case	Parameter	Units	Min. Value	Max. Value
I	D_{eff} Inventory	$[m^2 \cdot s^{-1}]$ [MTHM]	10^{-8} 10^{-4}	10^{-5} 10^1

Table 2 : Case I varied the reference diffusivity and waste inventory together. This dual parameter simulation case had 40 simulation groups of 100 realizations each.

		Mass Factor				
		0.001	0.01	0.1	1	10
		Groupings				
Reference Diffusivity (m^2/s)	1.E-08	1	2	3	4	5
	1.E-09	6	7	8	9	10
	1.E-10	11	12	13	14	15
	1.E-11	16	17	18	19	20
	1.E-12	21	22	23	24	25
	1.E-13	26	27	28	29	30
	1.E-14	31	32	33	34	35
	1.E-15	36	37	38	39	40

Table 3 : Diffusion coefficient and mass factor simulation groupings.



Case I : Diffusion Coefficient and Inventory

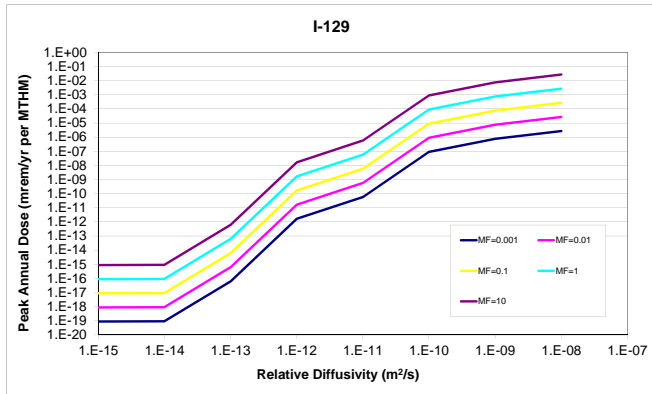


Figure 4 : The peak doses due to highly soluble, non-sorbing elements such as *I* are largely directly proportional to the relative diffusivity.



Case I : Diffusion Coefficient and Inventory

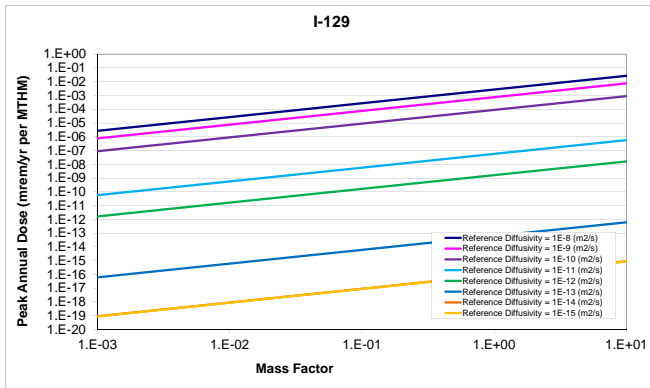


Figure 5 : The peak doses due to highly soluble, non-sorbing elements such as I are proportional to the radionuclide inventory.



Case I : Diffusion Coefficient and Inventory

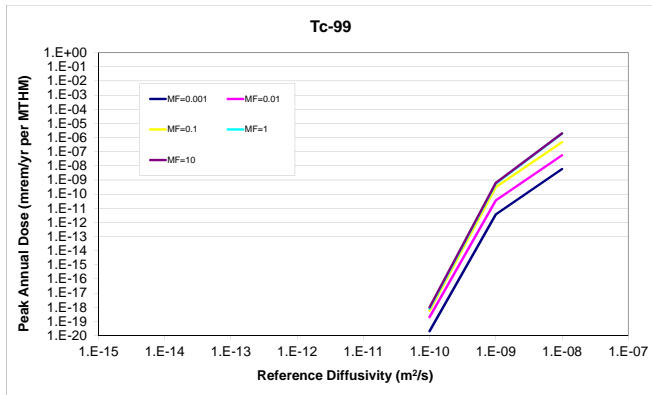


Figure 6 : ^{99}Tc relative diffusivity sensitivity.



Case I : Diffusion Coefficient and Inventory

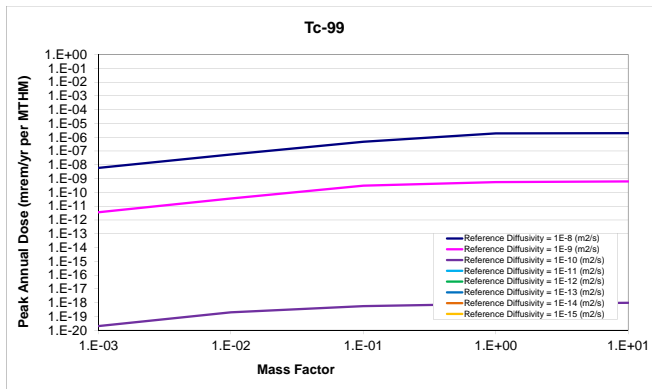


Figure 7 : ^{99}Tc mass factor sensitivity.



Case II : Vertical Advective Velocity and Diffusion Coefficient

Advection is transport driven by bulk water velocity while diffusion is the result of Brownian motion across concentration gradients. The method by which the dominant solute transport mode (diffusive or advective) is determined for a particular porous medium is by use of the dimensionless Peclet number,

$$\begin{aligned}Pe &= \frac{nvL}{\alpha nv + D_{eff}}, \\&= \frac{\text{advective rate}}{\text{diffusive rate}}\end{aligned}\tag{3}$$

where

n = solute accessible porosity [%]

v = advective velocity [$m \cdot s^{-1}$]

L = transport distance [m]

α = dispersivity [m]

D_{eff} = effective diffusion coefficient [$m^2 \cdot s^{-1}$].

For a high Pe number, advection is the dominant transport mode, while diffusive or dispersive transport dominates for a low Pe number [7].



Case II : Vertical Advective Velocity and Diffusion Coefficient

Simulation Cases

Case	Parameter	Units	Min. Value	Max. Value
II	$V_{adv,y}$	$[m \cdot yr^{-1}]$	6.31×10^{-8}	6.31×10^{-4}
	D_{eff}	$[m^2 \cdot s^{-1}]$	10^{-8}	10^{-5}

Table 4 : Case II varied the advective velocity and effective diffusivity to determine the nature of the threshold between the diffusive and advective regimes. This dual parameter simulation case had 40 simulation groups of 100 realizations each.

The forty runs are a combination of the five values of the vertical advective velocity and eight magnitudes of relative diffusivity.

		Vertical Advective Velocity [m/yr]				
		6.31E-08	6.31E-07	6.31E-06	6.31E-05	6.31E-04
		Groupings				
Reference Diffusivity (m ² /s)	1.E-08	1	2	3	4	5
	1.E-09	6	7	8	9	10
	1.E-10	11	12	13	14	15
	1.E-11	16	17	18	19	20
	1.E-12	21	22	23	24	25
	1.E-13	26	27	28	29	30
	1.E-14	31	32	33	34	35
	1.E-15	36	37	38	39	40



Case II : Vertical Advective Velocity and Diffusion Coefficient

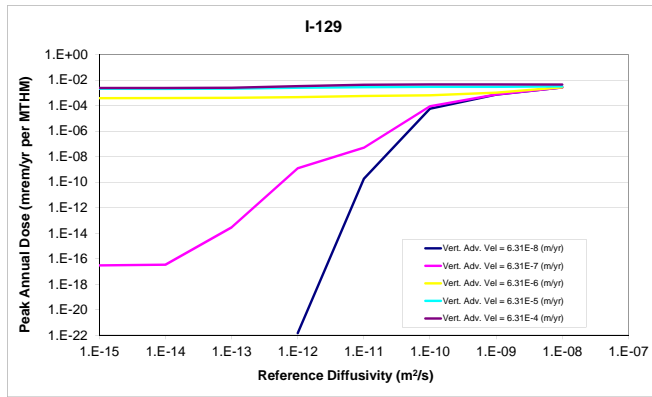


Figure 8 : ^{129}I . For vertical advective velocities $6.31 \times 10^{-6} [\text{m/yr}]$ and above, lower reference diffusivities are ineffective at attenuating the mean of the peak doses for soluble, non-sorbing elements.



Case II : Vertical Advective Velocity and Diffusion Coefficient

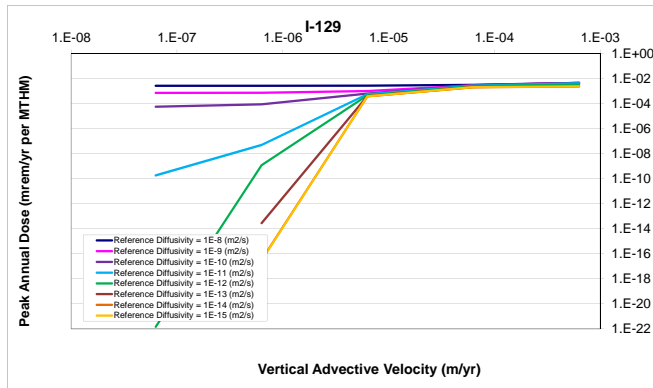


Figure 9 : I^{129} . For vertical advective velocities $6.31 \times 10^{-6} [m/yr]$ and above, lower reference diffusivities are ineffective at attenuating the mean of the peak doses for soluble, non-sorbing elements.



Case II : Vertical Advective Velocity and Diffusion Coefficient

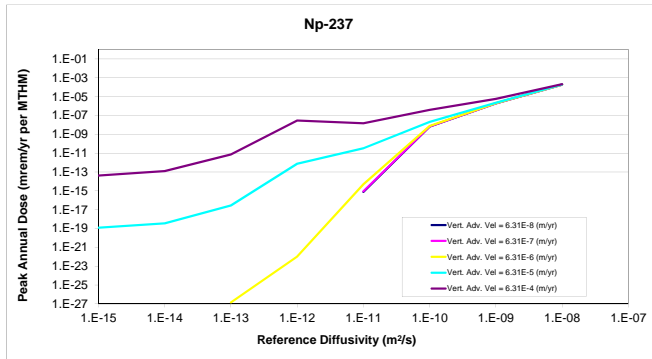


Figure 10 : ^{237}Np . shows a very weak influence on peak annual dose rate for low reference diffusivities, but a direct proportionality between dose and reference diffusivity above a threshold.



Case II : Vertical Advective Velocity and Diffusion Coefficient

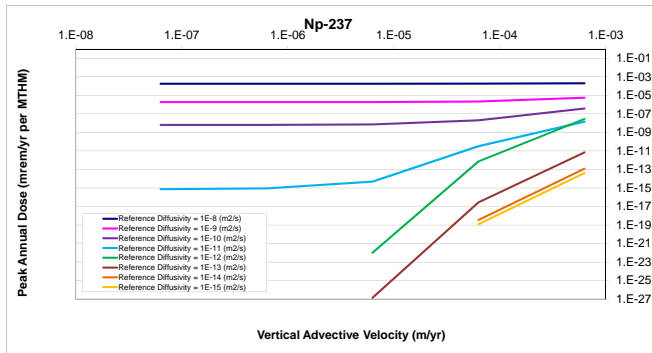


Figure 11 : ^{237}Np . shows a very weak influence on peak annual dose rate for low reference diffusivities, but a direct proportionality between dose and reference diffusivity above a threshold.



Case II : Vertical Advective Velocity and Diffusion Coefficient

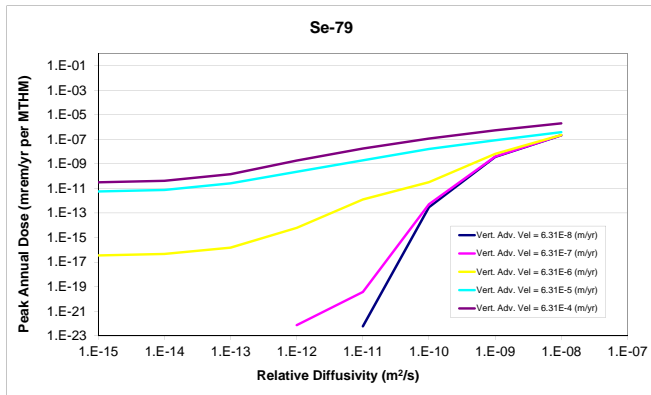


Figure 12 : ^{79}Se . Se is non sorbing, but solubility limited. For low vertical advective velocity, the system is diffusion dominated.



Case II : Vertical Advective Velocity and Diffusion Coefficient

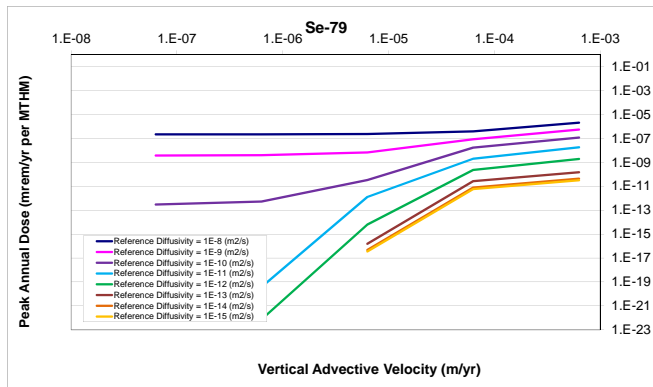


Figure 13 : ^{79}Se . Se is non sorbing, but solubility limited. For high vertical advective velocity, the diffusivity remains important even in the advective regime as spreading facilitates transport in the presence of solubility limited transport. vertical advective velocity sensitivity.



Case III : Solubility Coefficient

The reference solubilities for each element were multiplied by the multiplier for each simulation group. This technique preserved relative solubility among elements.

Simulation Cases

Case	Parameter	Units	Min. Value	Max. Value
III	S_i	$[mol \cdot m^{-3}]$	$(1 \times 10^{-9})\langle S_i \rangle$	$(5 \times 10^{10})\langle S_i \rangle$

Table 6 : Case III varied a solubility factor across many magnitudes. This single parameter simulation case had 40 simulation groups of 100 realizations each.



Case III : Solubility Coefficient

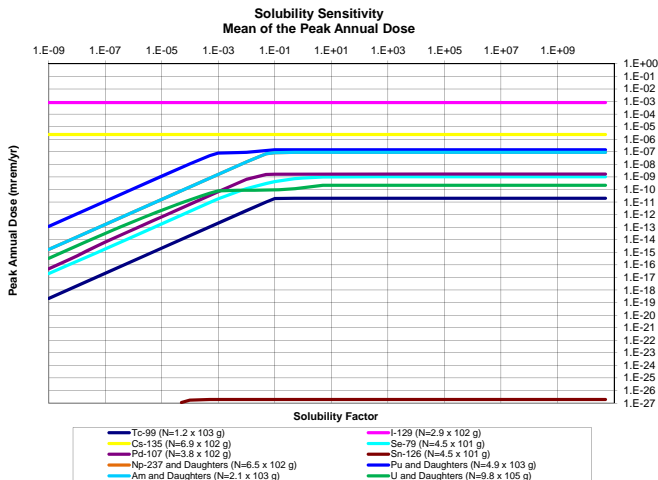


Figure 14 : The peak annual dose due to an inventory, N , of each isotope. For solubility constants lower than the inventory threshold, the relationship between peak annual dose and solubility limit is strong.



Case IV : Partition Coefficient

The retardation factor, R_f , which is the ratio between velocity of water through a volume and the velocity of a contaminant through that volume, can be expressed in terms of the partition coefficient,

$$R_f = 1 + \frac{\rho_b}{n_e} K_d \quad (4)$$

where

$$\rho_b = \text{bulk density} [kg \cdot m^{-3}]$$

and

$$n_e = \text{effective porosity of the medium [\%].}$$

The coefficient K_d , in units of $[m^3 \cdot kg^{-1}]$, is the ratio of the mass of contaminant in the solid to the mass of contaminant in the solution.



Case IV : Partition Coefficient

The parameters in this model were all set to the default values except a multiplier applied to the partitioning K_d coefficients.

Simulation Cases

Case	Parameter	Units	Min. Value	Max. Value
IV	$K_{d,i}$	$[m^3 \cdot kg^{-1}]$	$(1 \times 10^{-9})\langle K_{d,i} \rangle$	$(5 \times 10^{10})\langle K_{d,i} \rangle$

Table 7 : Case IV varied the partitioning coefficient, K_d , multiplication factor. This single parameter simulation case had 40 simulation groups of 100 realizations each.



Case IV : Partition Coefficient

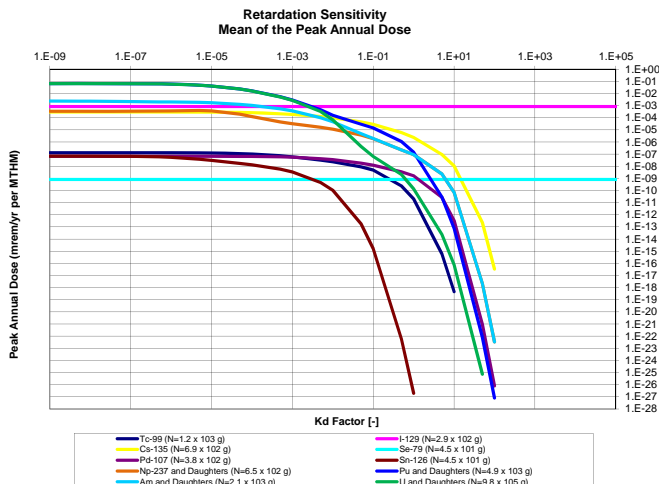


Figure 15 : For retardation coefficients greater than a threshold, the relationship between peak annual dose and retardation coefficient is a strong inverse one.



Case IV : Partition Coefficient

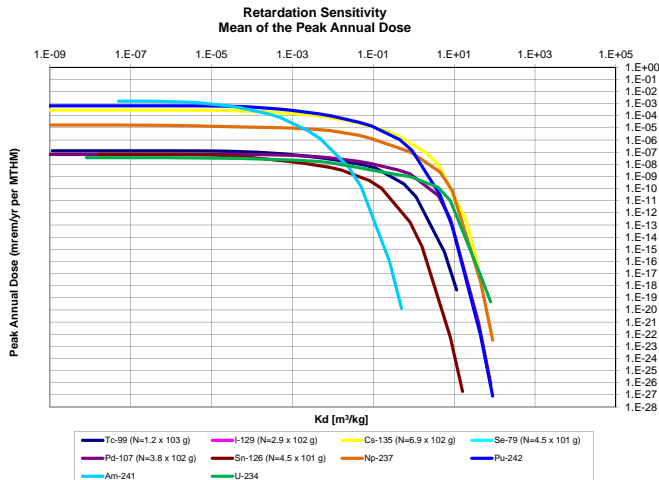


Figure 16 : For retardation coefficients greater than a threshold, the relationship between peak annual dose and retardation coefficient is a strong inverse one.



Case V : Waste Form Degradation Rate and Inventory

These runs varied the waste form degradation rate and the waste inventory mass factor. There were forty runs corresponding to eight values of the waste form degradation rate and five values of the mass factor.

Simulation Cases

Case	Parameter	Units	Min. Value	Max. Value
V	$R_{WFDeg.}$ Inventory	[yr^{-1}] [MTHM]	10^{-9} 10^{-4}	10^{-2} 10^1

Table 8 : Case V simultaneously varied the rate of waste form degradation and the waste form inventory mass factor. This dual parameter simulation case had 40 simulation groups of 100 realizations each.



Case V : Waste Form Degradation Rate and Inventory

Safety indicators for post closure repository performance have been developed by the UFD campaign which utilize the inventory multiplier that was varied in this study [6]. These indicators are normalized by a normalization factor (100 mrem/yr) recommended by the International Atomic Energy Agency (IAEA) as the limit to "relevant critical members of the public" [1]. The functional form for this safety indicator for a single waste category, high level waste (HLW), is just

$$SI_G = \left(\frac{\sum_{i=1}^N D_{G,i}(I_i, F_d)}{100 \text{mrem/yr}} \right) [\text{GWe/yr}]. \quad (5)$$

where

SI_G = Safety indicator for disposal in media type G[GWe/yr]

N = Number of key radionuclides considered in this indicator

$D_{G,i}$ = Peak dose rate from isotope i in media type G[mrem/yr]

F_d = Fractional waste form degradation rate[1/yr].



Case V : Waste Form Degradation Rate and Inventory

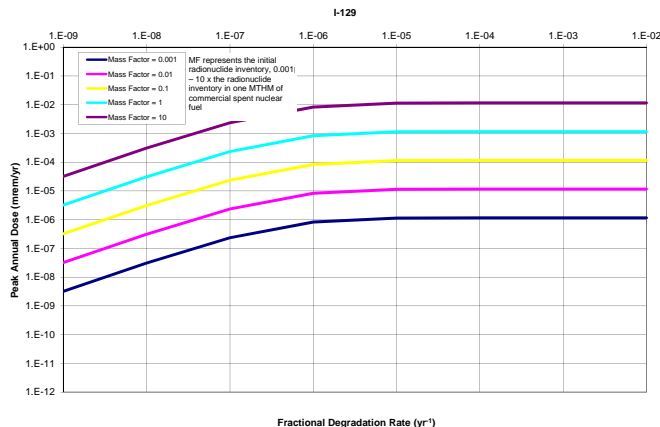


Figure 17 : Highly soluble and non-sorbing ^{129}I demonstrates a direct proportionality between dose rate and fractional degradation rate until a turnover where other natural system parameters dampen transport.



Case V : Waste Form Degradation Rate and Inventory

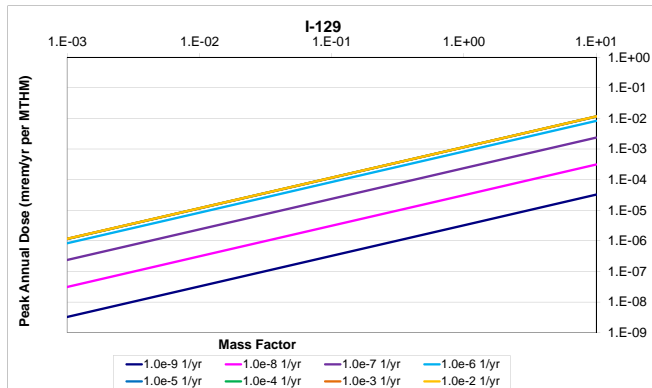


Figure 18 : Highly soluble and non-sorbing ^{129}I demonstrates a direct proportionality to the inventory multiplier.



Case V : Waste Form Degradation Rate and Inventory

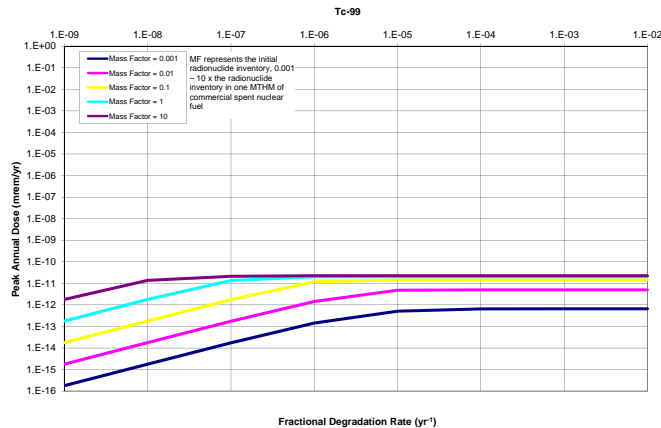


Figure 19 : Solubility limited and sorbing ^{99}Tc demonstrates a stronger turnover and direct proportionality to fractional degradation rate until attuation by its solubility limit and other natural system parameters.



Case V : Waste Form Degradation Rate and Inventory

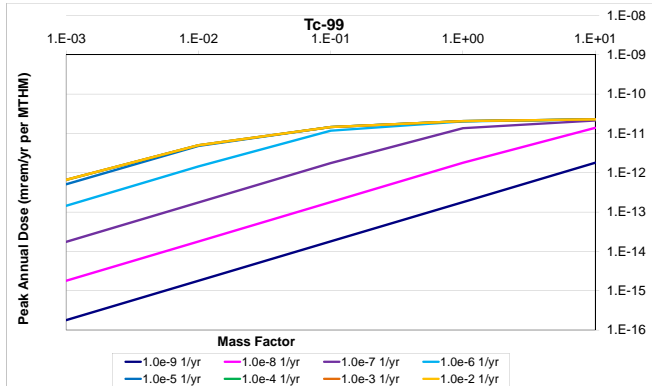


Figure 20 : Solubility limited and sorbing ^{99}Tc demonstrates a direct proportionality to fractional degradation rate until attuation by its solubility limit and other natural system parameters.



Case V : Waste Form Degradation Rate and Inventory

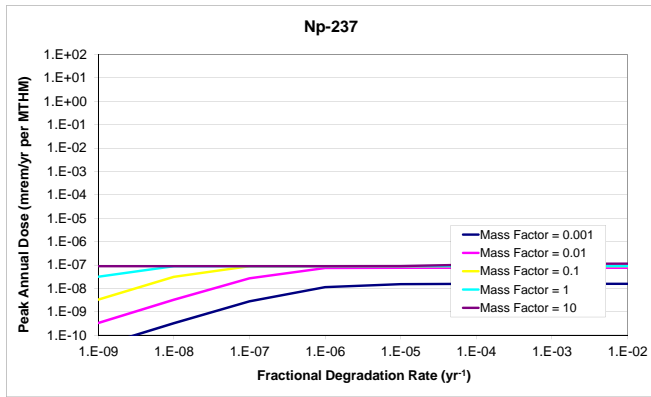


Figure 21 : Solubility limited and sorbing ^{237}Np demonstrates a direct proportionality to fractional degradation rate until attuation by its solubility limit and other natural system parameters.



Case V : Waste Form Degradation Rate and Inventory

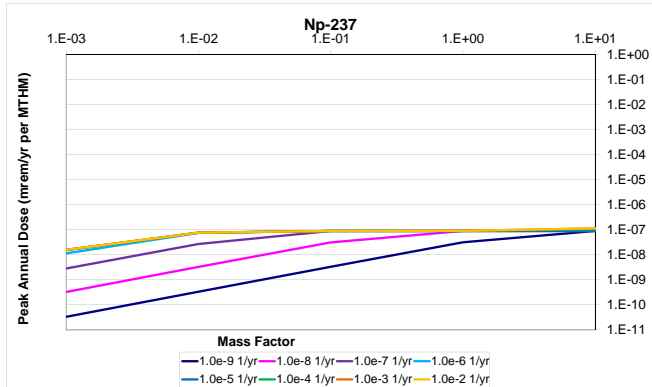


Figure 22 : Solubility limited and sorbing ^{237}Np demonstrates a direct proportionality to fractional degradation rate until attuation by its solubility limit and other natural system parameters.



Case VI : Waste Package Failure Time and Diffusion Coefficient

To investigate the effect of the waste package failure time, it was varied over five magnitudes from one thousand to ten million years. Simultaneously, the reference diffusivity was varied over the eight magnitudes between 1×10^{-8} and 1×10^{-15} in order to determine the correlation between increased radionuclide mobility and the waste package lifetime.

Simulation Cases

Case	Parameter	Units	Min. Value	Max. Value
VI	t_{WPFail} D_{eff}	[yr] $[m^2 \cdot s^{-1}]$	10^3 10^{-8}	10^7 10^{-5}

Table 9 : Case IV simultaneously varied the time of waste package failure and the reference diffusivity. This dual parameter simulation case had 40 simulation groups of 100 realizations each.



Case VI : Waste Package Failure Time and Diffusion Coefficient

For the clay repository, the waste package failure time is entirely irrelevant until waste package failure times reach the million or ten million year time scale.

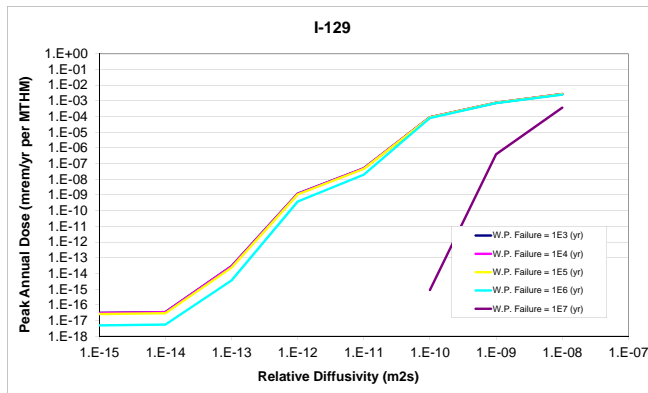
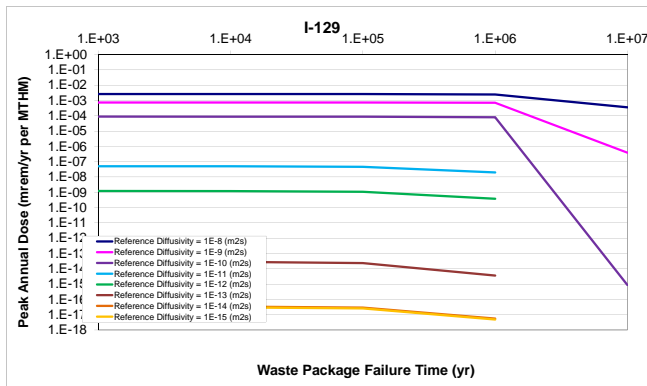


Figure 23 : ^{129}I / waste package failure time sensitivity.



Case VI : Waste Package Failure Time and Diffusion Coefficient

Figure 24 : ^{129}I waste package failure time sensitivity.



Outline

① Introduction

② Results

③ Summary



Summary of Sensitivity Analyses

In the Clay GDSM,

- the threshold between the advective and diffusive regimes was found outside of the expected parametric range for a clay repository,
- solubility and sorption characteristics of dose contributing elements have a strong effect on the importance of dispersion and advection parameters,
- waste form degradation rates over $1 \times 10^{-8}[\text{yr}]$ are also ineffective at decreasing the mean of the peak annual dose,
- waste package lifetimes under one million years are ineffective at decreasing the mean of the peak annual dose.



Acknowledgements

This work is supported by the U.S. Department of Energy, Basic Energy Sciences, Office of Nuclear Energy, under contract # DE-AC02-06CH11357.



References |

- [1] International basis safety standards for protection against ionizing radiation and the safety of radiation sources.
Technical Report 115, International Atomic Energy Agency, Vienna, Austria, July 1996.
- [2] D Clayton, G Freeze, E Hardin, W.M. Nutt, J Birkholzer, H.H. Liu, and S Chu.
Generic disposal system modeling - fiscal year 2011 progress report.
Technical Report FCRD-USED-2011-000184,SAND2011-5828P, U.S. Department of Energy,
Sandia, NM, August 2011.
- [3] Golder Associates.
GoldSim Contaminant Transport Module.
GoldSim Technology Group, version 6.0 edition, December 2010.
- [4] Golder Associates.
GoldSim Graphical Simulation Environment User's Guide.
GoldSim Technology Group, version 5.1 edition, January 2010.
- [5] S. Gonzales and K. S Johnson.
Shales and other argillaceous strata in the United States.
1985.



References II

- [6] W. Mark Nutt, Edgar Morris, Yifeng Wang, Lee Joon, Carlos Jove-Colon, and Shaoping Chu.
Generic repository concept analyses to support the establishment of waste form performance requirements.
Technical Report GNEP-WAST-PMO-MI-DV-2008-000146, US-DOE-NE Separations and Waste Form Campaign, July 2009.
- [7] F. W. Schwartz and H. Zhang.
Fundamentals of ground water.
Environmental Geology, 45:10371038, 2004.
- [8] W. von Lensa, R. Nabbi, and M. Rossbach.
RED-IMPACT Impact of Partitioning, Transmutation and Waste Reduction Technologies on the Final Nuclear Waste Disposal.
Forschungszentrum Julich, 2008.